nature cell biology

Activation of ATM depends on chromatin interactions occurring before induction of DNA damage

Yong-Chul Kim[1,6], Gabi Gerlitz[1,6], Takashi Furusawa[1], Frédéric Catez[1,5], Andre Nussenzweig[2], Kyu-Seon Oh[3], Kenneth H. Kraemer[3], Yosef Shiloh[4] and Michael Bustin[1,7]

Efficient and correct responses to double-stranded breaks (DSB) in chromosomal DNA are crucial for maintaining genomic stability and preventing chromosomal alterations that lead to cancer[1,2]. The generation of DSB is associated with structural changes in chromatin and the activation of the protein kinase ataxia-telangiectasia mutated (ATM), a key regulator of the signalling network of the cellular response to DSB[3,4]. The interrelationship between DSB-induced changes in chromatin architecture and the activation of ATM is unclear[4]. Here we show that the nucleosome-binding protein HMGN1 modulates the interaction of ATM with chromatin both before and after DSB formation, thereby optimizing its activation. Loss of HMGN1 or ablation of its ability to bind to chromatin reduces the levels of ionizing radiation (IR)-induced ATM autophosphorylation and the activation of several ATM targets. IR treatments lead to a global increase in the acetylation of Lys 14 of histone H3 (H3K14) in an HMGN1-dependent manner and treatment of cells with histone deacetylase inhibitors bypasses the HMGN1 requirement for efficient ATM activation. Thus, by regulating the levels of histone modifications, HMGN1 affects ATM activation. Our studies identify a new mediator of ATM activation and demonstrate a direct link between the steady-state intranuclear organization of ATM and the kinetics of its activation after DNA damage.

It is now clear that the action of chromatin modifiers that are recruited to DSB sites has an important role in the DNA damage response and the repair of these lesions[5,6]; however, the chain of events linking the generation of DSB to architectural changes in chromatin and activation of ATM are still not fully understood. Recent electron microscopy studies revealed that generation of DSB leads to a rapid, ATP-dependent, local decondensation of chromatin that occurs in the absence of ATM activation[7], supporting the suggestion that architectural changes in chromatin may be involved in the initiation of the DNA damage response[8]. In addition, ATM mediates transient, global chromatin decondensation through phosphorylation of the KAP-1 protein[9]. The local and global changes in chromatin organization facilitate recruitment of damage-response proteins and remodelling factors, which further modify chromatin in the vicinity of the DSB and propagate the DNA damage response. Given the extensive changes in chromatin structure associated with the DSB response, it could be expected that architectural chromatin-binding proteins, such as the high mobility group (HMG) proteins, would be involved in this process[10–12].

HMG is a superfamily of nuclear proteins that bind to chromatin without any obvious specificity for a particular DNA sequence and affect the structure and activity of the chromatin fibre[10,12,13]. We have previously reported that HMGN1, an HMG protein that binds specifically to nucleosome core particles, affects the repair of DNA damaged by either UV[14] or IR[15]. *Hmgn1*$^{-/-}$ mice and mouse embryonic fibroblasts (MEFs) are hypersensitive to IR and have an increased tumorigenic potential[15].

As DSB are critical DNA lesions induced by IR, and as ATM is the main transducer of the DSB response, we tested whether HMGN1 is involved in IR-induced ATM activation. A convenient marker of mouse ATM activation is its autophosphorylation on Ser 1987 (ref. 16). Analyses of IR-treated primary MEFs isolated from wild-type and *Hmgn1*$^{-/-}$ littermates revealed that loss of HMGN1 does not affect the ATM level, but significantly reduces the IR-induced autophosphorylation of Ser 1987 (Fig. 1a). Loss of HMGN1 also reduced the IR-induced phosphorylation of p53, and reduced the levels of both p53 and MDM2 (Fig. 1b). Similarly, loss of HMGN1 reduced the IR-induced phosphorylation of SMC1, CHK1 and CHK2 (Supplementary Information, Fig. S1), all of which are ATM targets[3].

To verify that IR-induced ATM activation is indeed HMGN1-dependent, we tested stable transformants of *Hmgn1*$^{-/-}$ cells ectopically expressing HMGN1 under the control of the tetracycline promoter (cell line no. 622). Before HMGN1 induction, only minor ATM autophosphorylation on Ser 1987 was detected after IR, but doxycycline-induced expression of physiological levels of HMGN1 elevated both IR-dependent autophosphorylation of ATM (Fig. 1c) and p53 phosphorylation and stabilization (Fig. 1d).

[1]Laboratory of Metabolism, [2]Experimental Immunology Branch and [3]Basic Research Laboratory, CCR, National Cancer Institute, National Institutes of Health, Bethesda, MD 20892, USA. [4]Department of Human Molecular Genetics and Biochemistry, Sackler School of Medicine, Tel Aviv University, Tel Aviv 69978, Israel. [5]Current address: Université Lyon 1, Lyon, F-69003, France; CNRS, UMR5534, Centre de génétique moléculaire et cellulaire, Villeurbanne, F-69622, France. [6]These authors contributed equally.
[7]Correspondence should be addressed to M.B. (e-mail: bustin@helix.nih.gov)

Received 29 August 2008; accepted 8 October 2008; published online 14 December 2008; DOI: 10.1038/ncb1817

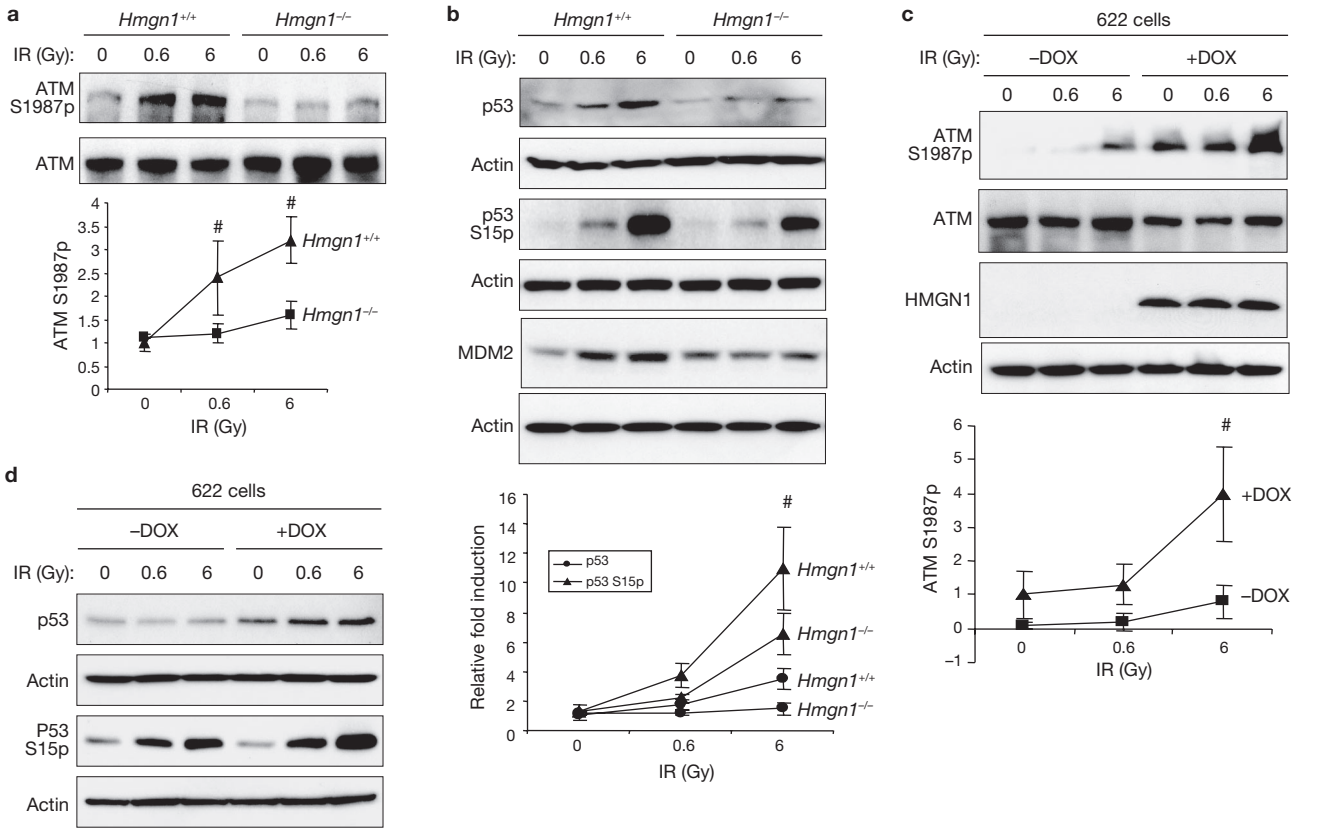

Figure 1 Loss of HMGN1 impairs IR-induced ATM autophosphorylation and activation. (**a**) Western blot analyses with the indicated antibodies in IR-treated *Hmgn1*$^{+/+}$ and *Hmgn1*$^{-/-}$ MEFs from littermate mice. The graph shows the mean ± s.d. of five independent experiments with MEFs prepared from different sets of littermates. (**b**) Impaired damage-induced p53 stabilization and MDM2 activation in *Hmgn1*$^{-/-}$ cells. Western blot analysis was carried out on extracts from IR-treated MEFs with the indicated genotypes. The graph show the mean ± s.d. of three independent experiments with MEFs prepared from different sets of littermates. (**c**) Rescue of ATM activation by re-expression of HMGN1. *Hmgn1*$^{-/-}$ MEFs stably transformed with a doxycyline (Dox)-inducible vector expressing ectopic HMGN1 (cell line no. 622) were irradiated and extracts analysed by western blotting with the indicated antibodies. Dox treatment (2 μg ml^{-1}, 48 h) induces HMGN1 expression and rescues ATM autophosphorylation. The graph show the mean ± s.d. of three independent experiments. (**d**) Rescue of p53 activation by re-expressing HMGN1. Experimental details are as in **c**. $^{\#}P < 0.05$, Student's *t*-test (**a**, **b**, **c**).

A key event in the cellular response to DSB is accumulation of sensors, such as Mre11, Rad50 and Nbs1 (the MRN complex), MDC1 and 53BP1, at the damaged sites[17–22]. Formation of these multiprotein complexes at DSB sites facilitates activation of ATM and amplification of the damage signal. Since in living cells HMGN1 molecules are in constant motion and continuously exchange among chromatin binding sites[23,24], we tested whether HMGN1 accumulates at the damaged sites and affects recruitment of the damage sensory proteins. Immunofluorescence microscopy analyses and examination of live cells expressing HMGN1–GFP indicated that IR treatment did not affect the intracellular distribution of HMGN1, and the protein did not accumulate at the break sites (Supplementary Information, Fig. S2a, b). Similarly, IR-induced formation of Nbs1, MDC1, 53BP1 and γH2AX foci in *Hmgn1*$^{-/-}$ cells was similar to that of wild-type MEFs (Supplementary Information, Fig. S3). Thus, the reduced ATM activation in *Hmgn1*$^{-/-}$ cells is not due to faulty recruitment of DSB sensors to the damaged sites.

These results raised the possibility that the impaired ATM activation in *Hmgn1*$^{-/-}$ cells is related to the interaction of ATM with chromatin, which is consistent with the suggestion that changes in chromatin structure activate ATM even in the absence of DSB[8]. To examine this possibility, we used an established 'chromatin retention assay'[25] to follow IR-induced recruitment of ATM to chromatin. As expected, in *Hmgn1*$^{+/+}$ cells, induction of DSB led to a 3-fold increase in the level of chromatin-bound ATM (Fig. 2, fraction III and graph). Surprisingly, before IR, the levels of chromatin-bound ATM were already twofold higher in *Hmgn1*$^{-/-}$ than in *Hmgn1*$^{+/+}$ cells, and DSB induction further increased by 3-fold the amount of chromatin-bound ATM in *Hmgn1*$^{-/-}$ cells (Fig. 2). Consistent with previous data[26], ATM Ser 1987p was detected mainly in the chromatin-bound fraction of the irradiated cells and loss of HMGN1 decreased the levels of this modification. Hence, loss of HMGN1 increases the amount of chromatin-bound ATM but reduces the amount of ATM Ser 1987p, thus resulting in a relative phosphorylation level (ATM Ser 1987p/ATM) of ATM that was at least 4 times lower than that in *Hmgn1*$^{-/-}$ cells (Fig. 2).

HMGN1 is a structural protein that binds specifically to nucleosome core particles and affects DNA-dependent activities, such as transcription and repair, but only in the context of chromatin[13,23]. HMGN1 mutants that do not bind to chromatin affect neither UV- nor IR-mediated DNA repair[14,15]. To test whether the effects of HMGN1 on ATM activation are contingent on chromatin binding, we compared the IR-induced levels of ATM Ser 1987p in *Hmgn1*$^{-/-}$ cells expressing wild-type HMGN1 protein (cell line no. 622) with cells expressing a double-mutant HMGN1S20,24E (cell line no. M101), which localizes to the nucleus but does not bind to chromatin[23]. Ectopic expression of wild-type HMGN1, but not of the HMGN1S20,24E mutant, elevated DSB-dependent ATM autophosphorylation at Ser 1987 and activation of p53 (Fig. 3). We therefore conclude

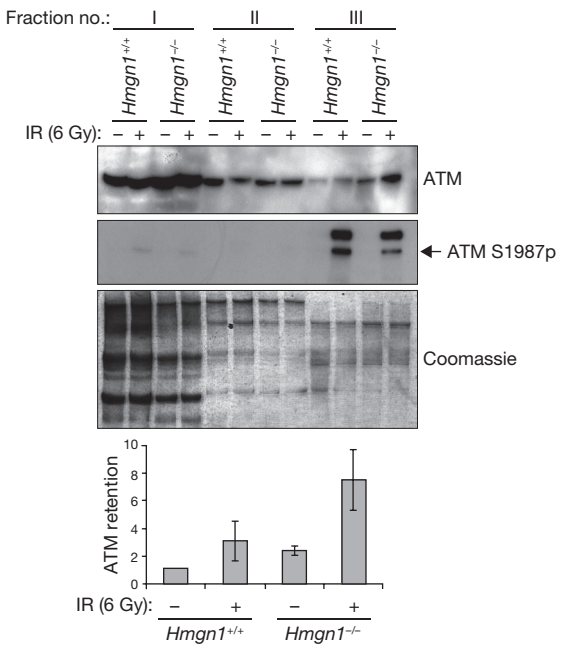

Figure 2 Enhanced ATM chromatin retention in *Hmgn1*$^{-/-}$ cells. Littermate *Hmgn1* $^{+/+}$ and *Hmgn1*$^{-/-}$ MEFs were fractionated 1 h after mock treatment or irradiation with 6 Gy. Equal numbers of cells from the soluble fraction (I), the washing fraction (II) and from the chromatin enriched fraction (III) were analysed by western blotting for ATM and ATM Ser 1987p levels. Coomassie blue staining of a parallel gel shows equal loading of protein. The bar graphs represent the relative levels of ATM retained on chromatin as the mean ± s.d. of three independent experiments. The retained ATM level in non-irradiated *Hmgn1*$^{+/+}$ cells was set at 1.

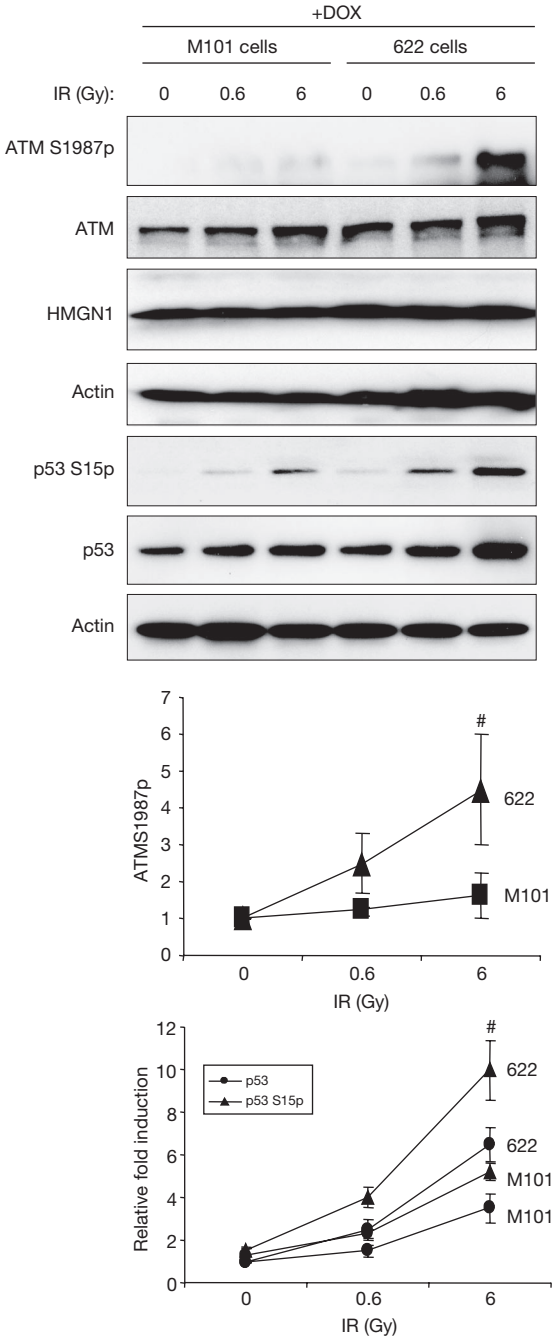

Figure 3 HMGN1 enhances ATM activation by binding to chromatin. *Hmgn1*$^{-/-}$ MEFs stably transformed with a doxycyline (Dox)-inducible vector expressing either wild-type HMGN1 (cell line no. 622) or the mutant HMGN1 S20,24E (M101cells), which does not bind to chromatin, were irradiated and extracts analysed by westerns with the indicated antibodies. The graphs represent the mean ± s.d. of three independent experiments; $^{\#}P < 0.05$, Student's *t*- test.

that the interaction of HMGN1 with chromatin enhances ATM activation. However, immunofluorescence microscopy analyses revealed that HMGN1 does not colocalize with ATM, an indication that ATM does not bind to chromatin regions containing HMGN1 (Supplementary Information, Fig. S4). Thus, the impaired activation of ATM in *Hmgn1*$^{-/-}$ cells is due to global changes in chromatin organization rather than to loss of a specific interaction between HMGN1 and ATM.

The interaction of HMGN1 with nucleosomes alters not only the 'higher order' chromatin structure, but also the local accessibility of histone tails to modifying enzymes and therefore the levels of several histone post-translational modifications in *Hmgn1*$^{-/-}$ cells are different from those in wild-type MEFs[27,28]. Alterations in the levels of histone modifications are known to have an important role in DSB repair[5,29,30]. We therefore hypothesized that HMGN1 affects ATM activation through modulation of histone modifications. To test this possibility, we investigated whether IR alters the levels of modifications in the tail of histone H3, at positions known to be affected by HMGN1. Western blotting and immunofluorescence microscopy analyses (Fig. 4a, b) revealed that IR treatment enhanced the global acetylation of H3K14 in *Hmgn1*$^{+/+}$, but less so in *Hmgn1*$^{-/-}$, thereby providing support for our hypothesis. As a further test of the link between HMGN1-mediated histone modification and ATM activation, we examined whether elevation of histone acetylation levels by an HDAC inhibitor, before IR treatment, would simulate the effect of HMGN1 on ATM activation. MEFs derived from *Hmgn1*$^{-/-}$ and *Hmgn1*$^{+/+}$ littermate mice were incubated with HDAC inhibitors, exposed to IR and ATM autophosphorylation levels were determined (Fig. 4c). In *Hmgn1*$^{+/+}$ cells, pre-incubation with HDAC inhibitors increased the IR-induced ATM phosphorylation levels by approximately 20% (Fig. 4c). Significantly, in cells lacking HMGN1, pre-incubation with HDAC inhibitors elevated the levels of IR-induced ATM autophosphorylation by 2-fold. As a result, the relative phosphorylation levels of HDAC-treated *Hmgn1*$^{-/-}$ cells were indistinguishable from those of the wild-type cells (Fig. 4c).

Our finding that incubation of cells with an HDAC inhibitor before IR exposure simulates the effects of HMGN1, together with the observation that the absence of HMGN1 protein increases chromatin retention of ATM

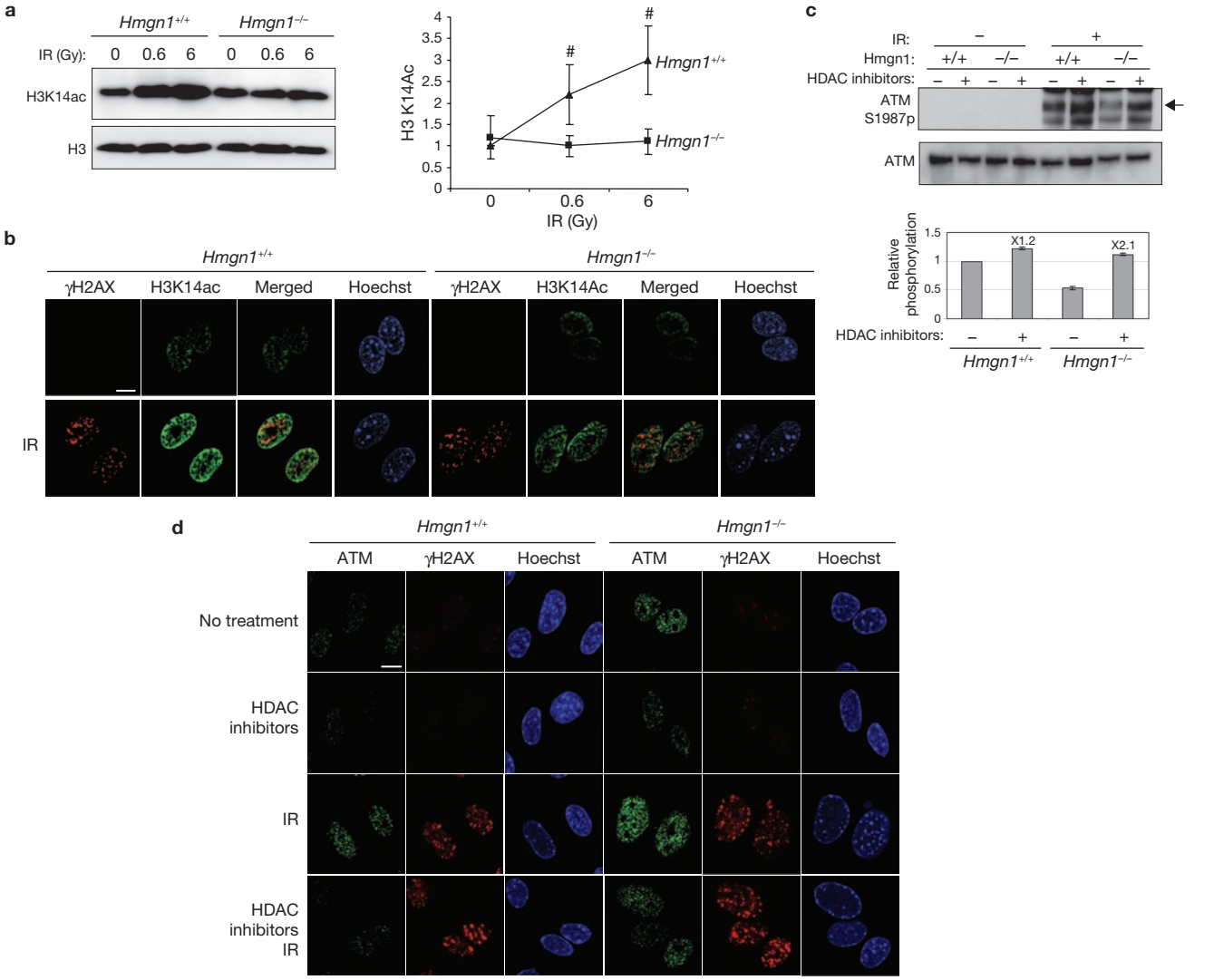

Figure 4 HMGN1 modulates the interaction of ATM with chromatin. (**a**) Loss of HMGN1 reduces IR-induced acetylation of Lys 14 in histone H3. Shown is a western blot analysis of H3K14ac in IR-treated *Hmgn1*$^{-/-}$ and *Hmgn1*$^{+/+}$ MEFs. The graphs represent calculated the mean ± s.d. of three independent experiments; $^{\#}P < 0.05$, Student's *t*-test. (**b**) IR-induced acetylation of H3K14 is HMGN1-dependent and not limited to the DNA breakage points. Shown are confocal images of immunostaining with antibodies to H3K14ac and γH2AX in IR-treated *Hmgn1*$^{-/-}$ and *Hmgn1*$^{+/+}$ MEFs. Note that the H3K14ac in *Hmgn1*$^{+/+}$ cells is more intense than in *Hmgn1*$^{-/-}$cells. Scale bar is 10 μm. (**c**) Enhanced histone acetylation before IR treatment abrogates the effect of *Hmgn1*$^{-/-}$ on ATM activation. Shown are western blot analyses of the levels of ATM and ATM Ser 1987p in *Hmgn1*$^{-/-}$ and *Hmgn1*$^{+/+}$ MEFs that were incubated with or without the HDAC inhibitors trichostatin A (0.5 μg ml^{-1}) and sodium butyrate (2 mM) for 4 h before exposure to 6 Gy of IR. The bar graph represents ATM activation as the ratio between autophosphorylated and total ATM (ATM Ser 1987p/ATM), obtained by quantifying the western blot signals (mean ± s.d.) from three independent experiments. The ratio for irradiated *Hmgn1*$^{+/+}$ cells that were not exposed to the HDAC inhibitors was set at 1. (**d**) Enhanced histone acetylation before IR treatment abrogates the effect of HMGN1 on ATM chromatin binding. *Hmgn1*$^{-/-}$ and *Hmgn1*$^{+/+}$ MEFs were either treated or not with HDAC inhibitors, exposed to 6 Gy of IR and pre-lysed on ice before paraformaldehyde fixation. The fixed cells were immunostained with antibodies against ATM and γH2AX. DNA was stained with Hoechst. Scale bar is 10 μm

even without IR treatment (Fig. 2), raises the possibility that HMGN1 affects the intranuclear organization of ATM. Indeed, *in situ* ATM retention assays revealed increased ATM retention in *Hmgn1*$^{-/-}$ cells both before and after IR treatment (Fig. 4d). Significantly, HDAC inhibitors reduced the levels of chromatin-bound ATM both before and after IR exposure (Fig. 4d). ATM activation has been linked to its acetylation[31]; however, we found that after HDAC treatment, acetylation of ATM in IR-treated *Hmgn1*$^{-/-}$ cells was not higher than in similarly treated *Hmgn1*$^{+/+}$ cells (Supplementary Information, Fig. S5). Thus, HMGN1 enhances IR-induced activation of ATM by elevating the acetylation levels of nucleosomal histones. Although HMGN1 affects IR-dependent ATM phosphorylation, it does not significantly alter UV-irradiation-dependent ATM phosphorylation (Supplementary Information, Fig. S6).

In summary, our results suggest that the activation dynamics of ATM are affected by chromatin interactions that occur before IR-induced generation of DSB. ATM retention assays with purified chromatin, immunofluorescence microscopy analyses of permeabilized cells and analyses of HDAC-inhibited cells (Figs 2, 4c, d) all demonstrate that a fraction of ATM is associated with chromatin before IR treatment and that loss of HMGN1 increases this fraction. These results, together with the findings that

HMGN mutants that do not bind chromatin do not affect ATM activation (Fig. 3), and that HMGN1 does not accumulate at DSB (Supplementary Information, Fig. S2), suggest that by modifying chromatin, HMGN1 affects the global organization of ATM throughout the nucleus and not only at the DSB sites (Fig. 4d). Thus, the properties of the chromatin fibre predetermine the cellular response to IR-induced DNA damage.

METHODS

Preparation of primary MEFs and MEF cell lines. Primary *Hmgn1*$^{+/+}$ and *Hmgn1*$^{-/-}$ MEFs, and transformed MEF cells stably expressing either wild-type or mutant HMGN1 protein under the control of the Tet promoter were described previously[14]. □

Irradiation and antibodies for western blotting. Cells were incubated in 10-mm dishes until confluent within 70–80% for irradiation. The cells were exposed to ionizing radiation from a ^{137}Cs Shepherd Mark II irradiator at a cumulative dose of 0.6 and 6Gy. After irradiation, the cells were incubated for 1 h. For western blotting, the cells were scraped and washed with PBS buffer. Then cell lysates were prepared for sonication with 1 × SDS sample buffer (62.5 mM Tris-HCl at pH 6.8, 2% SDS, 10% glycerol, 50 mM DTT), heated to 95 °C for 5 min and centrifuged for 5 min. The proteins were separated by SDS–PAGE and transferred to PVDF membranes. The following antibodies were used for western blotting: CHK1 (G-4), lot A2403, 1:500 (Santa Cruz Biotechnology); pATM (Ser 1987) lot 17858, 1:400; pSMC1 (Ser 957) lot 14411, 1:100 (Rockland); p53, lot 4, 1:500; SMC1, lot 1, 1:500; pp53 (Ser 15) lot 6, 1:1,000; pCHK1 (Ser 345) lot 1, 1:500 (Cell Signaling); H3K14ac, lot 30020, 1:2,000; CHK2, lot 22186, 1:400 (Upstate); HMGN1, 1:3,000; histone H3, 1:20,000 (ref. 14); MAT3 anti ATM[25], 1:1,000. The same membranes were re-blotted for anti-non-phospho-antibodies and β-actin antibodies (1:5,000; Sigma) to control the amounts of protein loaded.

Immunostaining analysis. For foci formation, control or X-ray-irradiated MEFs plated on glass coverslips were further incubated for 30 min or 16 h at 37 °C. After fixation in methanol at –20 °C for 20 min, the cells were washed three times with PBS and blocked in PBS–BSA (1% BSA in PBS) at room temperature for 1 h. The cells were labelled with antibodies against MDC1, 1:1,1000; Nbs1, 1:1,000 (ref. 32); 53BP1, 1:500 (Novus Biologicals) and γH2AX, lot 32526, 1:2,000 (Upstate) for 1 h at room temperature, washed three times with PBS and labelled with secondary antibodies; Cy3-fused donkey anti-rabbit, 1:200, or FITC-fused donkey anti-mouse, 1:150 (Jackson ImmunoResearch Laboratories) for 1 h at room temperature. After three washings with PBS, the DNA was stained with Hoechst 33258 (Molecular Probes) and the coverslips were mounted using Vectashield mounting medium (H-1000, Vector Laboratories). For H3K4ac, cells were fixed with 3% paraformaldehyde in PBS for 20 min at room temperature, treated with 0.1% triton in PBS for 10 min and immunostained as described above.

ATM retention assay. The ATM retention assay was modified from a previous report[25]. Briefly, for biochemical fractionation, MEFs grown to 60–70% confluence in 15-cm plates were collected, washed twice with PBS and the cell pellets resuspended in 150 μl of buffer I (50 mM HEPES at pH 7.6, 150 mM NaCl, 1 mM EDTA, 0.25% Triton X-100, 0.5 μg ml^{-1} TSA, protease inhibitor cocktail, phosphatase inhibitor cocktail 1 and 2 (Sigma)). After a 5-min incubation on ice and 5-min centrifugation at 1000*g* at 4 °C, the supernatants were collected (fraction I), the pellets were washed once with 150 μl buffer I and the supernatants were collected (fraction II). Following addition of 150 μl of SDS sample buffer, the nuclei pellets were sonicated and boiled for 5 min (fraction III). Equal volumes from the different fractions were separated on 5% SDS–PAGE and immunoblotted for ATM and pATM (Ser 1987). For *in situ* retention, control or X-ray-irradiated MEFs grown on glass coverslips were incubated for a further 1 h at 37 °C and placed on ice. After one wash with ice-cold PBS, the coverslips were incubated twice in buffer I supplemented with 1% Triton X-100 for 10 min each. Next, the cells were fixed in 3% paraformaldehyde in PBS at room temperature for 20 min and immunostained with antibodies against ATM (H248, Santa Cruz Biotechnology) and γH2AX. The DNA was stained with Hoechst 33258.

Note: Supplementary Information is available on the Nature Cell Biology website.

ACKNOWLEDGEMENTS

We thank A. Celeste (NCI) for advice and help, and S. Garfield (Confocal Core Facility of the LEC, NCI), for help with imaging. The research was supported by the intramural program of the NCI. Work in the laboratory of Y.S. is supported by the A-T Medical Research Foundation, the A-T Children's Project, The Israel Science Foundation, the A-T Medical Research Trust, the Israel-Germany Joint Program on Cancer Research, and the A-T Ease Foundation.

COMPETING FINANCIAL INTERESTS

The authors declare no competing financial interests.

Published online at http://www.nature.com/naturecellbiology/
Reprints and permissions information is available online at http://npg.nature.com/reprintsandpermissions/

1. Mills, K. D., Ferguson, D. O. & Alt, F. W. The role of DNA breaks in genomic instability and tumorigenesis. *Immunol. Rev.* **194,** 77–95 (2003).
2. Hoeijmakers, J. H. Genome maintenance mechanisms for preventing cancer. *Nature* **411,** 366–374 (2001).
3. Shiloh, Y. The ATM-mediated DNA-damage response: taking shape. *Trends Biochem Sci.* **31,** 402–410 (2006).
4. Lavin, M. F. & Kozlov, S. ATM activation and DNA damage response. *Cell Cycle* **6,** 931–942 (2007).
5. Wurtele, H. & Verreault, A. Histone post-translational modifications and the response to DNA double-strand breaks. *Curr. Opin. Cell Biol.* **18,** 137–144 (2006).
6. Koundrioukoff, S., Polo, S. & Almouzni, G. Interplay between chromatin and cell cycle checkpoints in the context of ATR/ATM-dependent checkpoints. *DNA Repair* **3,** 969–978 (2004).
7. Kruhlak, M. J. *et al.* Changes in chromatin structure and mobility in living cells at sites of DNA double-strand breaks. *J. Cell Biol.* **172,** 823–834 (2006).
8. Bakkenist, C. J. & Kastan, M. B. DNA damage activates ATM through intermolecular autophosphorylation and dimer dissociation. *Nature* **421,** 499–506 (2003).
9. Ziv, Y. *et al.* Chromatin relaxation in response to DNA double-strand breaks is modulated by a novel ATM- and KAP-1 dependent pathway. *Nature Cell Biol.* **8,** 870–876 (2006).
10. Hock, R., Furusawa, T., Ueda, T. & Bustin, M. HMG chromosomal proteins in development and disease. *Trends Cell Biol.* **17,** 72–79 (2007).
11. Reeves, R. & Adair, J. E. Role of high mobility group (HMG) chromatin proteins in DNA repair. *DNA Repair* **4,** 926–938 (2005).
12. Bianchi, M. E. & Agresti, A. HMG proteins: dynamic players in gene regulation and differentiation. *Curr. Opin. Genet. Dev.* **15,** 496–506 (2005).
13. Bustin, M. Regulation of DNA-dependent activities by the functional motifs of the high-mobility-group chromosomal proteins. *Mol. Cell Biol.* **19,** 5237–5246 (1999).
14. Birger, Y. *et al.* Chromosomal protein HMGN1 enhances the rate of DNA repair in chromatin. *EMBO J.* **22,** 1665–1675 (2003).
15. Birger, Y. *et al.* Increased tumorigenicity and sensitivity to ionizing radiation upon loss of chromosomal protein HMGN1. *Cancer Res.* **65,** 6711–6718 (2005).
16. Pellegrini, M. *et al.* Autophosphorylation at serine 1987 is dispensable for murine Atm activation in vivo. *Nature* **443,** 222–225 (2006).
17. Lee, J. H. & Paull, T. T. ATM activation by DNA double-strand breaks through the Mre11-Rad50-Nbs1 complex. *Science* **308,** 551–554 (2005).
18. Uziel, T. *et al.* Requirement of the MRN complex for ATM activation by DNA damage. *EMBO J.* **22,** 5612–5621 (2003).
19. Wang, B., Matsuoka, S., Carpenter, P. B. & Elledge, S. J. 53BP1, a mediator of the DNA damage checkpoint. *Science* **298,** 1435–1438 (2002).
20. DiTullio, R. A., Jr *et al.* 53BP1 functions in an ATM-dependent checkpoint pathway that is constitutively activated in human cancer. *Nature Cell Biol.* **4,** 998–1002 (2002).
21. Stewart, G. S., Wang, B., Bignell, C. R., Taylor, A. M. & Elledge, S. J. MDC1 is a mediator of the mammalian DNA damage checkpoint. *Nature* **421,** 961–966 (2003).
22. Goldberg, M. *et al.* MDC1 is required for the intra-S-phase DNA damage checkpoint. *Nature* **421,** 952–956 (2003).
23. Catez, F., Lim, J. H., Hock, R., Postnikov, Y. V. & Bustin, M. HMGN dynamics and chromatin function. *Biochem. Cell Biol.* **81,** 113–122 (2003).
24. Phair, R. D. & Misteli, T. High mobility of proteins in the mammalian cell nucleus. *Nature* **404,** 604–609 (2000).
25. Andegeko, Y. *et al.* Nuclear retention of ATM at sites of DNA double strand breaks. *J. Biol. Chem.* **276,** 38224–38230 (2001).
26. Lou, Z. *et al.* MDC1 maintains genomic stability by participating in the amplification of ATM-dependent DNA damage signals. *Mol. Cell* **21,** 187–200 (2006).
27. Lim, J. H. *et al.* Chromosomal protein HMGN1 modulates histone H3 phosphorylation. *Mol. Cell* **15,** 573–584 (2004).
28. Lim, J. H. *et al.* Chromosomal protein HMGN1 enhances the acetylation of lysine 14 in histone H3. *EMBO J.* **24,** 3038–3048 (2005).
29. Murr, R. *et al.* Histone acetylation by Trrap-Tip60 modulates loading of repair proteins and repair of DNA double-strand breaks. *Nature Cell Biol.* **8,** 91–99 (2006).
30. Celeste, A. *et al.* Histone H2AX phosphorylation is dispensable for the initial recognition of DNA breaks. *Nature Cell Biol.* **5,** 675–679 (2003).
31. Sun, Y., Jiang, X., Chen, S., Fernandes, N. & Price, B. D. A role for the Tip60 histone acetyltransferase in the acetylation and activation of ATM. *Proc. Natl Acad. Sci. USA* **102,** 13182–13187 (2005).
32. Difilippantonio, S. *et al.* Role of Nbs1 in the activation of the Atm kinase revealed in humanized mouse models. *Nature Cell Biol.* **7,** 675–685 (2005).

nature cell biology

DOI: 10.1038/ncb1817

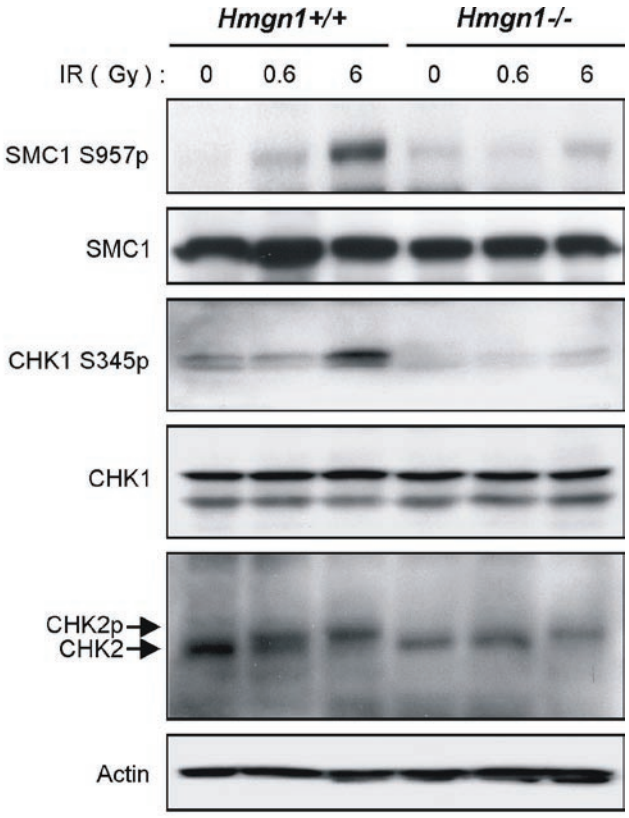

Figure S1 Impaired phosphorylation of ATM downstream targets in *Hmgn1*$^{-/-}$ MEFs. Shown are Western blots of extracts obtained from IR-treated MEFs with different *Hmgn1* genotypes, probed with the antibodies indicated. Chk2 phosphorylation is evident by its typical band-shift.

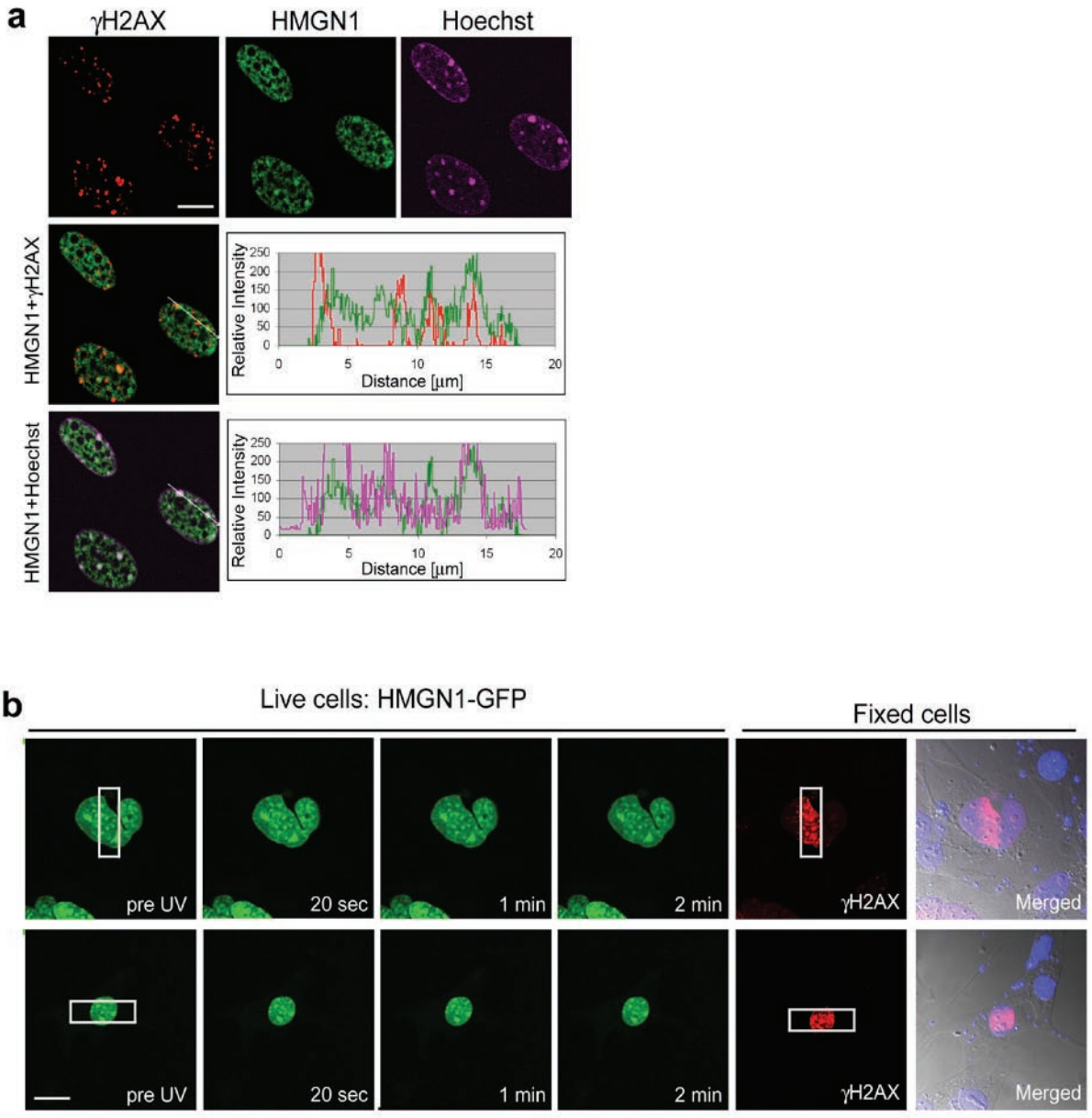

Figure S2 HMGN1 does not accumulate at DSB sites. (a) Immunofluorescence analysis of HMGN1 and phosphorylated H2AX in wild-type MEFs 1 h following irradiation of 6 Gy. Co-localization profiles of HMGN1 (green) and phosphorylated H2AX (red) as well as HMGN1 and DNA stained with Hoechst (purple) are shown. Scale bar is 10 μm. (b) Spatially confined DSBs were induced in cells expressing GFP-tagged HMGN1 using "laser scissors" exactly as described before [13]. The location of HMGN1- GFP was examined immediately after the treatment and followed up to 30 minutes using time-lapse photography, at which time they were fixed and stained for phosphorylated H2AX and for DNA with Hoechst. Two examples are shown. Scale bar is 10 μm.

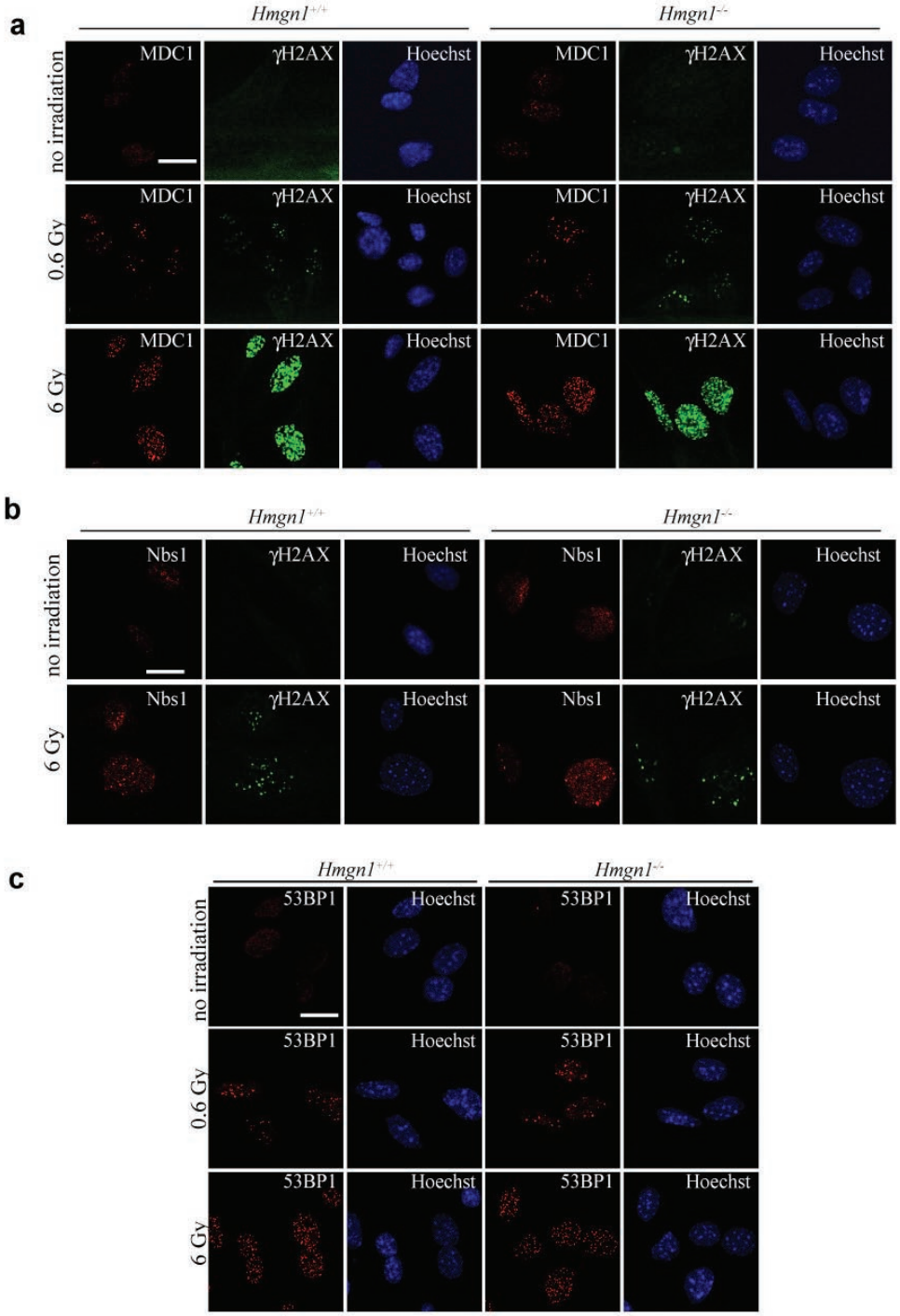

Figure S3 Loss of HMGN1 does not affect the accumulation of damage response proteins and the phosphorylation of H2AX at DSB sites. Immunofluorescence analysis of MDC1, Nbs1, 53BP1 and γH2AX was carried out in IR-treated *Hmgn1*$^{+/+}$ and *Hmgn1*$^{-/-}$ littermate MEFs. Scale bar is 20 μm.

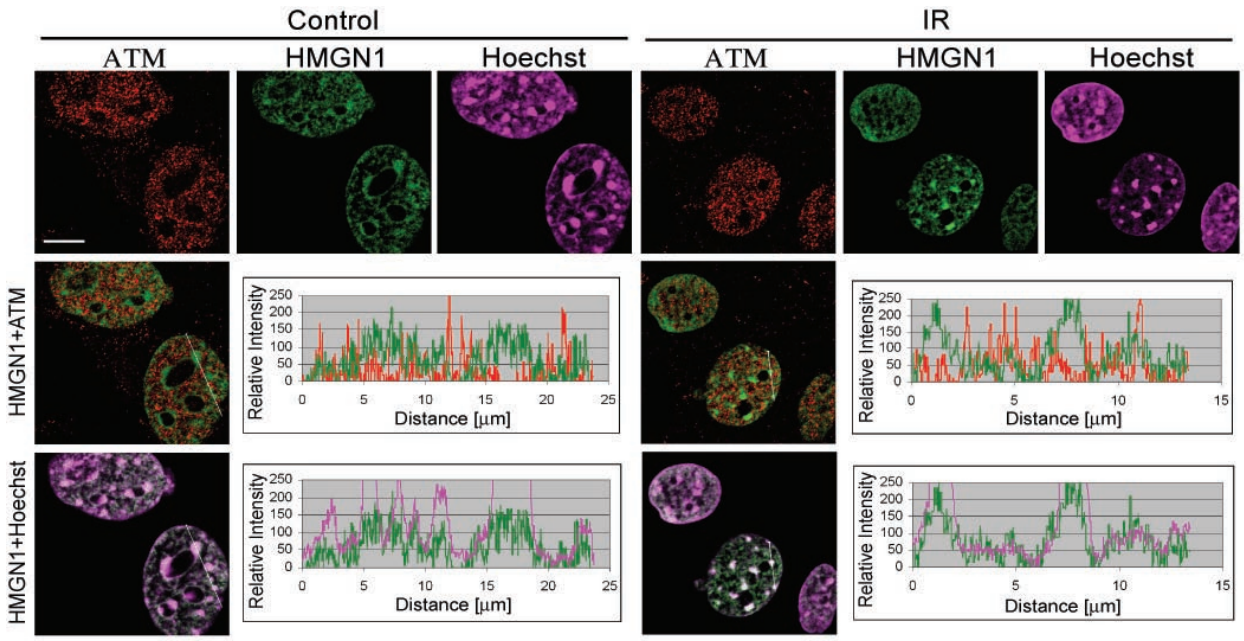

Figure S4 HMGN1 does not colocalize with ATM. Immunofluorescence analysis of HMGN1 and ATM in wild-type MEFs before and 1 h following irradiation of 6 Gy. Co-localization profiles of HMGN1 (green) and ATM (red) as well as HMGN1 and DNA as stained with Hoechst (purple) are shown. Scale bar is 10 μm.

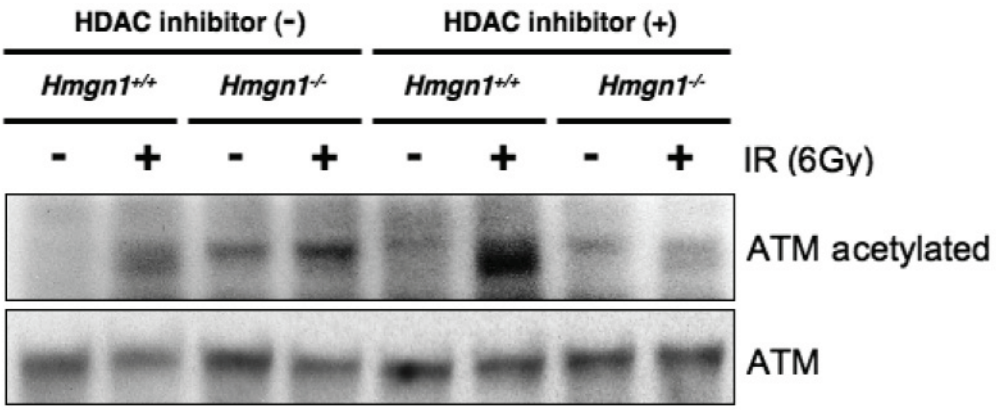

Figure S5 HDAC inhibitors-dependent recovery of ATM activation in cells lacking HMGN1 does not increase ATM acetylation. Shown are Western analyses of the levels of Ac-ATM and ATM in *Hmgn1*$^{-/-}$ and *Hmgn1*$^{+/+}$ MEFs that were incubated with or without 0.5 μg/ml of Trichostatin A and 2mM sodium butyrate (HDAC inhibitors) for 4 h prior to exposure to 6 Gy of IR.

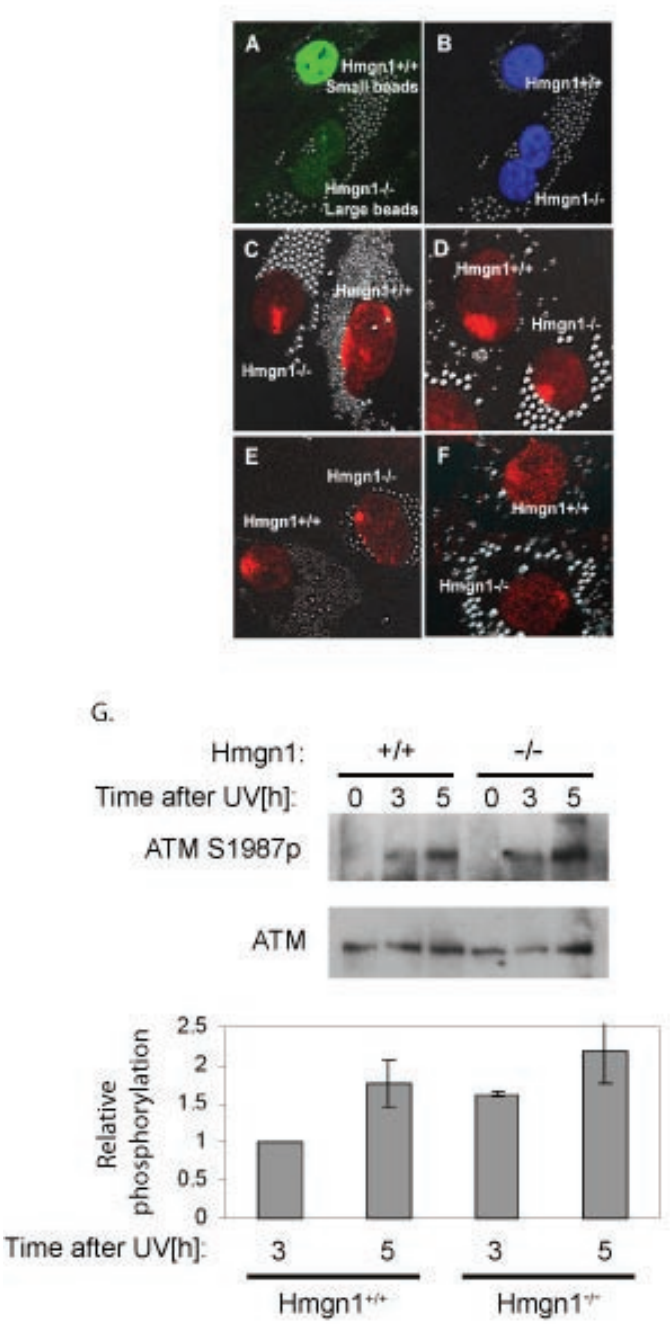

Figure S6 UV-induced phosphorylation of ATM in *Hmgn1*$^{-/-}$ and *Hmgn1*$^{+/+}$ MEFs. *Hmgn1*$^{-/-}$ and *Hmgn1*$^{+/+}$ MEFs were grown separately in the presence of beads of different size for 3-4 days (Jaspers, N.J, and Bootsma. D., Proc. Nat. Acad. Sci. 79, 2641-2644, 1982). *Hmgn1*$^{-/-}$ (2.0μm beads) and *Hmgn1*$^{+/+}$ (0.8μm beads) cells were cultured on the same slide for 1 day and then irradiated with 100J/m^2 UV-C through a 5μm pore size filter, cultured for 3 hours , fixed, and analyzed by immunofluorescence as described (Oh, K.S, et al., DNA repair, 6, 1359, 2007). A. Immunofluorescence analyses with antibodies to HMGN1 indicate that *Hmgn1*$^{+/+}$ cells are labeled with small beads while the *Hmgn1*$^{-/-}$ cells are labeled with large beads. B. Corresponding image stained with DAPI visualizes the nuclei of the cells. C, D. Staining with antibodies to cyclobutane pyrimidine dimers (Oh, K.S, et al., DNA repair, 6, 1359, 2007) visualizes the UV-damaged areas in the nuclei *Hmgn1*$^{-/-}$ and *Hmgn1*$^{+/+}$ cells . E, F. Staining of cells with antibodies to phospho-ATM reveals similar ATM activation in *Hmgn1*$^{-/-}$ and *Hmgn1*$^{+/+}$ cells. G. Western analysis of the levels of ATM and ATM S1987p in *Hmgn1*$^{+/+}$ and *Hmgn1*$^{-/-}$ MEFs that were incubated for 3 or 5 h after irradiation with 50 J/m^2 of UV-C. The cells at time 0 were not irradiated. The bar graph represents ATM activation as the ratio between autophosphorylated and total ATM (ATM S1987p/ATM), obtained by quantifying the Western signals. This ratio for *Hmgn1*$^{+/+}$ cells which were incubated for 3 h following the irradiation was set as 1.

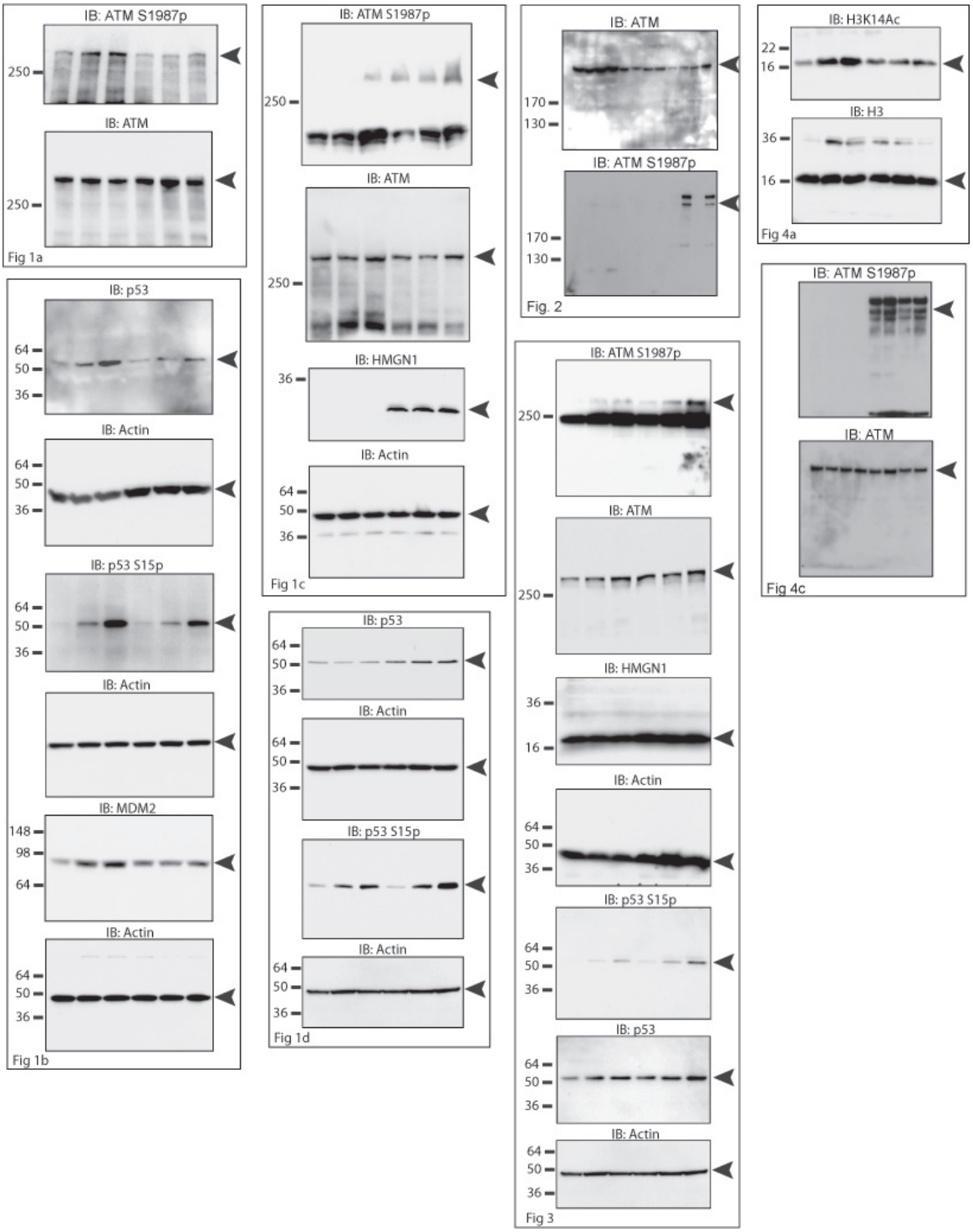

Figure S7 Full scans of western blot data